

# Metal oxide blended ZSM-5 nanocomposites as ethanol sensors

MADHURI LAKHANE<sup>1,2</sup>, RAJENDRA KHAIRNAR<sup>1</sup> and MEGHA MAHABOLE<sup>1,\*</sup>

<sup>1</sup>School of Physical Sciences, Swami Ramanand Teerth Marathwada University, Nanded (MS) 431606, India

<sup>2</sup>Faculty of Mechanical Engineering, University of Maribor, Maribor 2000, Slovenia

MS received 20 August 2015; accepted 21 March 2016

**Abstract.** Nano-ZSM-5 is synthesized without organic template via microwave-assisted hydrothermal technique. The synthesized nano-ZSM-5 zeolite is blended with metal oxides (ZnO and TiO<sub>2</sub>) to have novel composites as ethanol sensors. The composites are characterized by X-ray diffraction (XRD) and Fourier transform infrared (FTIR) techniques. A study on ethanol sensing behaviour of metal oxide blended composite screen-printed thick films is carried out and the effect of metal oxide concentration on various ethanol sensing features, specifically operating temperature, response/recovery time and active region of the sensor, are investigated. XRD and FTIR confirm the blending of metal oxides in ZSM-5 matrix. Both, ZnO and TiO<sub>2</sub> blended, composite films are sensitive to ethanol. It can be concluded that metal oxide blending improves the performance of sensor for ethanol detection. The response/recovery time and active sensing regions depend upon the concentration of metal oxide in host zeolite. The ZnO/ZSM-5 and TiO<sub>2</sub>/ZSM-5 composite films are the excellent ethanol sensors.

**Keywords.** ZSM-5 zeolite; composites; XRD; FTIR; ethanol sensing.

## 1. Introduction

Zeolite ZSM-5 [Na<sub>n</sub>Al<sub>n</sub>Si<sub>96-n</sub>O<sub>192</sub>·16H<sub>2</sub>O (0 < n < 27), abbreviated as Na-ZSM-5] is one of the most attractive members of high silica zeolite class. ZSM-5, a highly porous material, belongs to the pentasil family of zeolites with MFI framework [1]. Framework of ZSM-5 structure consists of intersecting 2D channel structure formed by 10-membered oxygen rings. The main characteristic of this framework structure is the presence of straight channels with elliptical cross-section and zig-zag patterned channels with circular cross-section. It is the channel diameter that determines catalytic activity, selectivity and stability of zeolite ZSM-5 and hence it is considered as a significant catalyst [2]. Combination of the various novel properties like unique structure, molecular-sieving behaviour, excellent ion exchange capacity and adsorption capabilities along with excellent high thermal stability and chemical resistance makes the ZSM-5 zeolite very favourable for sensor applications [3,4]. Moreover, the porous nature of ZSM-5 gives rise to the high surface area, due to which it provides numerous sites for adsorption of molecules to be sensed [5–7]. It is reported in the literature that zeolites can be employed in sensor field either as a host material or as a filter or thin layer to enhance the sensing properties, especially semiconducting materials based sensors [8]. Literature review also indicates that the zeolite structure can be modified by incorporating various transition metals, cations and metal oxides as the

guest molecules, by serving as a host. These modifications, in turn, strongly influence diffusion, catalytic and especially adsorption properties of zeolite and consequently influence sensing applications. Hence, these host guest interactions may be used as the basis for sensing [9–11].

Semiconductors are the most attractive materials for gas sensor applications. Among various semiconducting metal oxides, zinc oxide (ZnO) and titanium oxide (TiO<sub>2</sub>) have attracted much attention because of their excellent electronic, chemical and optical properties. It is due to numerous features like cost effectiveness and flexibility in production, simplicity, ease in implementation, small size, quick response/recovery and high sensitivity, these semiconductors are widely used as gas sensors [12]. Moreover, these oxides exhibit high temperature stability, harsh environment tolerance and catalytic properties. These oxide-based sensors can be employed for the detection of low concentration of reducing as well as oxidizing gases and give fast response to a wide variety of gases [13–15]. It is also reported in the literature that addition of TiO<sub>2</sub> to ZSM-5 leads to the increase in surface area [12].

Ethanol sensors, especially, have been the main focus of research in recent years for their applications in wide range of areas like chemical, biomedical and food industries, beverages quality monitoring, environmental monitoring, indoor air quality and breath analysis [16]. It is due to the great demand in diverse fields, that the search for new ethanol sensor materials is still needed. Literature survey reveals the sparseness in research based on metal oxide blended zeolite gas sensors.

Hence in this study, ZnO and TiO<sub>2</sub> metal oxides are incorporated into ZSM-5 matrix to have the novel metal oxide/zeolite composites to meet the requirement of desired

\*Author for correspondence (mpmsrtmunps@gmail.com, mahabolemegh@yahoo.co.in)

features, like high sensitivity, low working temperature and short response/recovery times for the ethanol sensor. The composite thick films, prepared by screen printing technique, are employed as the ethanol sensors and the effect of metal oxide concentration on ethanol sensing parameters is investigated.

## 2. Experimental

### 2.1 Materials

All the chemicals, used for synthesis of zeolite and fabrication of sensor, are of analytical grade purity and used without further purification. The raw materials used in this study, namely, sodium aluminate, sodium hydroxide, silica sol, titanium oxide ( $\text{TiO}_2$ ), zinc oxide ( $\text{ZnO}$ ) and silica sol, are procured from Merck, India.

### 2.2 Synthesis of Nano-ZSM-5 zeolite

ZSM-5 zeolite crystals are synthesized via microwave-assisted template-free hydrothermal method as per the method described in literature to reduce the synthesis time [17]. Sodium aluminate (aluminium source), sodium hydroxide and silica sol (silica source) are used as the starting chemicals to obtain synthesis sol. Initially, solution is prepared by dissolving simultaneously appropriate amounts of sodium hydroxide (4.0 g) and sodium aluminate (1.64 g) in 135 ml of deionized water. Silica sol (104 g) is slowly added to the solution under a condition of constant and vigorous stirring. Addition of silica sol immediately results in the formation of a white gel. The gel solution, thus formed, is further magnetically stirred for 5 h and later on aged for 24 h at room temperature for the first-order nucleation.

Prior to being transferred to a stainless steel autoclave, the aged gel is then exposed to microwave radiations for 5 min

to expedite the crystallization process and then transferred to autoclave. Finally, it is hydrothermally treated for variable time durations (20, 18, 15 and 12 h) at 453 K temperature in order to optimize crystallization period. After the completion of the reaction and series of experiments, the obtained products are air-cooled to room temperature. These products are further thoroughly washed with deionized water and filtered. All the obtained products are then dried at 373 K for 24 h and sintered at 773 K for 2 h. Synthesis protocol is presented in figure 1.

### 2.3 Preparation of metal oxide blended sensors

The main raw materials used for the sample preparation are zeolite and metal oxides. ZSM-5 zeolite is used as the host matrix and three different kinds of metal oxides are employed as the reinforcing guest molecules. The particle reinforced composites are prepared using nanoparticles of Merck grade metal oxides, namely,  $\text{ZnO}$ ,  $\text{TiO}_2$  and  $\text{CuO}$  with 25, 50 and 75% weight content of ZSM-5 zeolite using a simple physical mixture method. The ingredients are thoroughly dry mixed mechanically, using agate mortar, for about 10 h to have homogeneous admixtures and to ensure dispersion of metal oxides in zeolite at different concentrations.

### 2.4 Preparation of thick film sensors

The preparation of thick film sensor is as per the process reported earlier [18]. In brief, appropriate amount of prepared metal oxide/ZSM-5 composite is mixed and grounded with adhesive materials in an agate mortar to form a glutinous paste. The paste is then coated onto surface of pre-cleaned glass substrate by using screen printing technique to obtain thick films. Coated films are dried under IR lamp for 20 min followed by final sintering at  $650^\circ\text{C}$  for about 2 h for ensuring

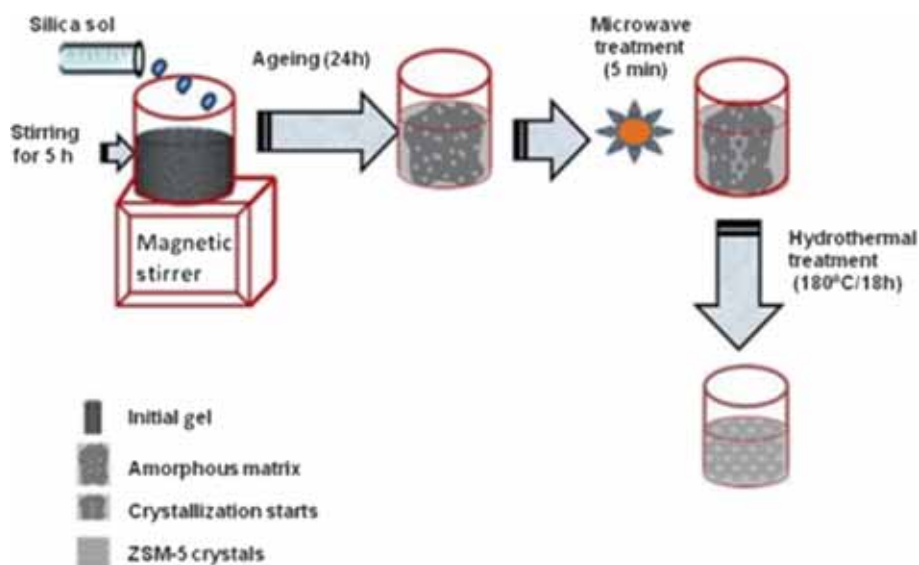


**Figure 1.** The synthesis protocol showing the growth process of nano-ZSM-5 zeolite.

proper adhesion of film. These films, thus prepared, are used to detect ethanol vapours.

### 2.5 Characterization

The crystallinity of the sintered ZSM-5 and metal oxide/ZSM-5 composites is verified by means of Rigaku-make X-ray diffractometer with Cu-K $\alpha$  radiation (1.54014 Å). The X-ray diffraction (XRD) peaks are recorded in the  $2\theta$  range of 5–60 degrees. Fourier transform infrared (FTIR) spectra of the ZSM-5 and prepared composite samples are recorded by means of KBr pellet technique in the FTIR scan range 4000–400  $\text{cm}^{-1}$  with a resolution of 4  $\text{cm}^{-1}$  using Shimadzu-make FTIR spectrophotometer.

### 2.6 Sensor performance testing method

Ethanol sensing performance of each developed sensor is tested by using a home-made static gas test unit. Briefly, the sensor is heated with the help of heater from room temperature to 350°C and sensor resistance is measured in air at an interval of 5°C temperature. Later on a fixed amount of ethanol (in p.p.m.) is injected into the test chamber through a gas inlet valve by using the syringe to have an ethanol vapour–air mixture followed by the measurement of resistance with respect to change in temperature. The sensing characteristics of the each sensor are determined by measuring the change in electrical resistance of the sensor film in air ( $R_a$ ) and in ethanol vapour–air mixture ( $R_g$ ). The response

to ethanol/sensitivity is calculated using the following equation [19]:

$$S(\%) = \frac{R_g - R_a}{R_a} \times 100, \quad (1)$$

where  $R_a$  is the resistance of sensor in air and  $R_g$  the resistance of sensor after ethanol exposure. The change in sensitivity of the film is plotted as a function of temperature and operating temperature is determined corresponding to a maximum sensitivity. The maximum ethanol uptake capacity of the sensor film is determined by exposing the film to variable ethanol concentrations (p.p.m.) and simultaneously measuring the change in resistance (sensitivity) as a function of variable ethanol concentration (p.p.m.). The time taken by the sensor to respond to a fixed ethanol vapour concentration (response time) and to regain its original state upon exposure to air (recovery time) are determined by exposing each composite film to air and fixed concentration of ethanol vapour–air mixture alternately.

## 3. Results and discussion

### 3.1 XRD studies

The XRD profiles of ZnO blended ZSM-5 composites are presented in figure 2A(a–d), wherein the XRD profile of pure ZSM-5 is considered as a reference. Figure 2A(a) reveals the presence of peaks corresponding to ZSM-5 zeolite structure

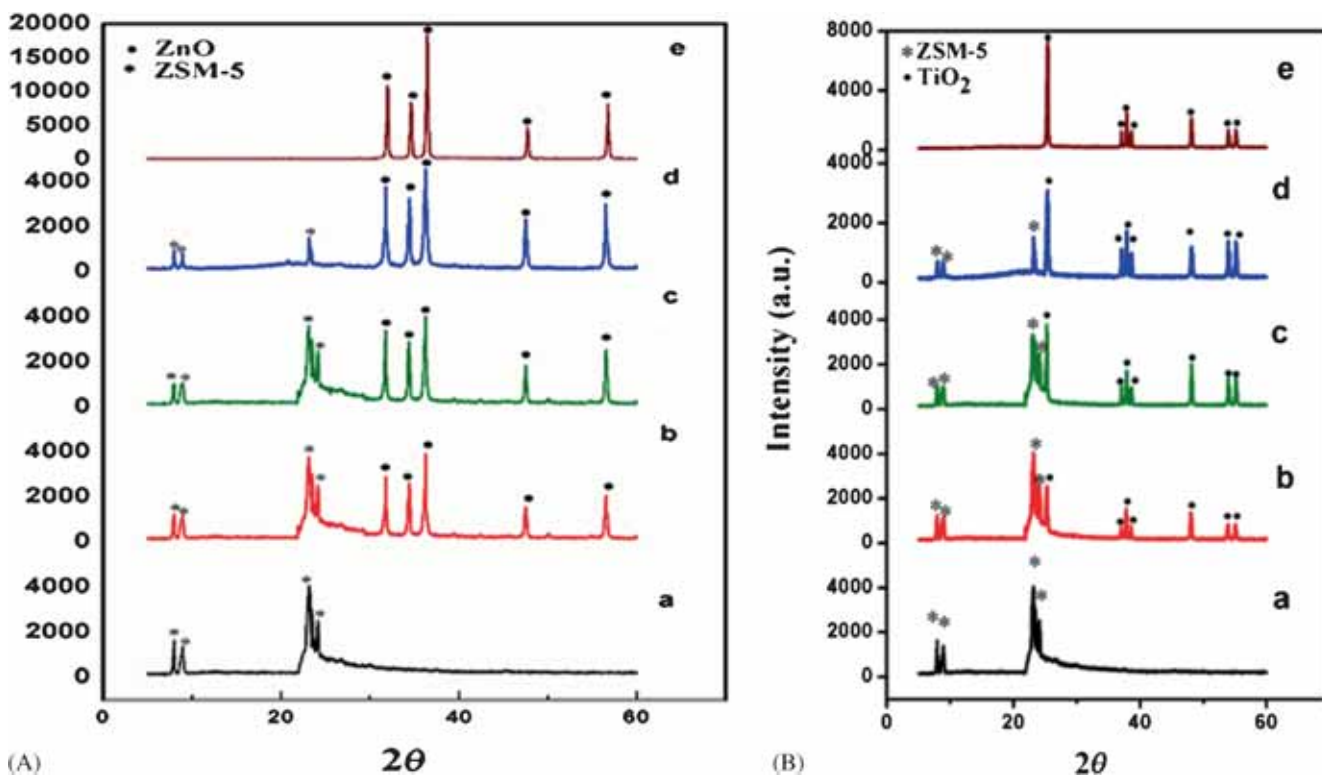


**Figure 2.** (A and B) Powder XRD patterns showing the presence of characteristic peaks of ZSM-5, ZnO and TiO<sub>2</sub>: (a) pure ZSM-5; (b) 25% metal oxide, (c) 50% metal oxide, (d) 75% metal oxide and (e) pure metal oxide.

[20]. The blending of ZnO with ZSM-5 zeolite host matrix can be visualized, from figure 2A(b–d), by the presence characteristic peaks of zinc oxide corresponding to (100), (002), (101), (102) and (110) planes. The phase analysis, carried out as per JCPDS card (36-1451), confirms the wurtzite-type hexagonal structure of ZnO. The intensities of ZnO planes are found to be increasing with increase in ZnO concentration in a composite. It is observed that the intensities of typical ZSM-5 peaks remain unaltered up to 50% ZnO contribution. However, for higher ZnO concentration (75%), sudden decrease in intensity is observed which indicates the dominance of ZnO in zeolite matrix. Moreover, sharp diffraction peaks apparent in all XRD profiles show good crystallinity of the pure as well as composite samples, and there are almost no changes in crystallinity of the zeolite composites.

Similar kind of behaviour is observed for TiO<sub>2</sub> blended ZSM-5 composites. Figure 2B(a–d) presents the XRD patterns for TiO<sub>2</sub> blended ZSM-5 zeolites as a function of TiO<sub>2</sub> concentration with that for pure ZSM-5 as the base. The XRD pattern shown in figure 2B(a) agrees well with that reported in the literature for ZSM-5 zeolite [21]. The presence of TiO<sub>2</sub> peaks near 2 $\theta$  values of 25.28, 37.9, 48.2, 53.8 and 55.2 degrees correspond to the anatase phase (JCPDS file no. 21-1272), as depicted in figure 2e. Figure 2B(b–d) reveals the presence of typical XRD peaks of host ZSM-5 matrix as well as reinforcing TiO<sub>2</sub>. It can be seen from figure 2B(b–d) that as the concentration of TiO<sub>2</sub> in composite increases, doublet nature of ZSM-5 peaks, appearing between 23 and 24°, changes to singlet and intensities for all ZSM-5 peaks decrease. Increase in TiO<sub>2</sub> concentration leads to increase in intensities of almost all peaks related to TiO<sub>2</sub> in all composite samples.

Thus, it can be concluded that XRD profiles of metal oxide blended ZSM-5 zeolite composite samples show their typical XRD peaks corresponding to ZnO, TiO<sub>2</sub> and ZSM-5 host. No new phase structure is detected. This indicates that the metal oxide particulates are scattered uniformly in the zeolite matrix and the blending of metal oxides do not destroy the structure of the zeolite.

### 3.2 FTIR spectroscopy

Figure 3A(a–d) shows the typical FTIR spectra of ZnO/ZSM-5 composites as a function of ZnO concentration and are compared with that of pure ZSM-5. The spectrum of pure ZSM-5 (figure 3A(a)) reveals the presence of typical bands corresponding to vibrations of tetrahedral and framework atoms in zeolite structure. The absorption peak at 482 cm<sup>-1</sup> can be attributed to bending vibrations of Si–O–Si bonds. The presence of this peak at 482 cm<sup>-1</sup> confirms the characteristic of five-membered ring pentasil structure of ZSM-5. A broad peak near 701 cm<sup>-1</sup> can be assigned to external symmetric stretching vibrations of Si–O group [22]. The absorption bands present at 898 and 1111 cm<sup>-1</sup> are attributed to external symmetric and internal asymmetric stretching vibrations of Si–O–Si bonds [20]. The structure sensitive absorption band (a small shoulder peak), attributed to asymmetric vibration of T–O bond corresponding to external linkages between TO<sub>4</sub> tetrahedra, is observed to be present at 1220 cm<sup>-1</sup> [23]. This peak is found to be disappearing for higher ZnO concentration (75%). The presence of weak band near 1590 cm<sup>-1</sup> corresponds to bending vibrations of adsorbed water molecules [22].

The IR spectrum of pure zinc oxide (figure 3A(e)) includes bands at 470 and 1111 cm<sup>-1</sup>. The band centred at 470 cm<sup>-1</sup> is due to the vibrations of Zn–O stretching modes. In the IR spectra of composites (figure 3A(b–d)), decrease in intensities of absorption bands at 482, 898 and 1111 cm<sup>-1</sup> attributed to ZSM-5 with increase in ZnO concentration. In case of composites, the peaks at 482 and 898 cm<sup>-1</sup> shift towards lower wavenumber side, i.e., at 470 and 860 cm<sup>-1</sup>, respectively. The characteristic feature of these spectra, compared with the spectra of pure ZSM-5 and ZnO, is the splitting of a broadband at 701 cm<sup>-1</sup> into doublet peaks. The emergence of new peak at 670 cm<sup>-1</sup> is related to stretching vibrations of Zn–O bond [24] and peak at 701 cm<sup>-1</sup> shifts at higher energy side. Moreover, the intensity of these doublet peaks also decreases with increase in the concentration of zinc oxide in the composites, while broadening the peaks. For the higher

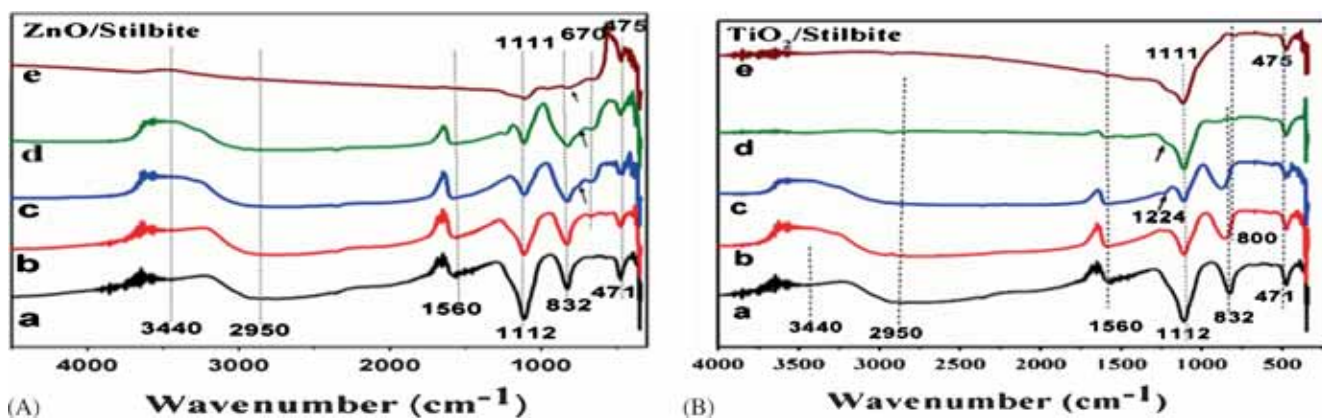


**Figure 3.** (A and B) Typical FTIR spectra of ZnO/ZSM-5 and TiO<sub>2</sub>/ZSM-5 composites depicting the existence of structure sensitive and insensitive absorption bands corresponding to various functional groups due to typical zeolite structure, ZnO and TiO<sub>2</sub>; (a) pure ZSM-5; (b) 25% metal oxide; (c) 50% metal oxide (d) 75% metal oxide and (e) pure metal oxide.

ZnO concentration, a small shoulder peak is observed at  $908\text{ cm}^{-1}$  which is also the characteristic peak of ZnO [25].

Figure 3B(a–e) displays FTIR spectra for pure ZSM-5 and  $\text{TiO}_2/\text{ZSM-5}$  composites and pure  $\text{TiO}_2$ . The FTIR spectrum, showing unique adsorption peaks corresponding to ZSM-5 structure, is considered as a reference. The spectrum of pristine titanium oxide (figure 3e) reveals the presence of absorption peaks at  $475$ ,  $800$  and  $1111\text{ cm}^{-1}$ . The bands at  $475$  and  $1111\text{ cm}^{-1}$  are due to Ti–O–Ti framework bonds [26]. The peak observed at  $800\text{ cm}^{-1}$  can be attributed to symmetric stretching vibration of Ti–O bonds in  $\text{TiO}_2$  lattice [27].

In the case of  $\text{TiO}_2/\text{ZSM-5}$  composite, inclusion of titanium oxide can be confirmed by the appearance of a new shoulder peak at  $800\text{ cm}^{-1}$ . The unique ZSM-5 peak present at  $880\text{ cm}^{-1}$  shifts to higher frequency side and the peak at  $1111\text{ cm}^{-1}$  slightly shifts towards low frequency. The peak occurring at  $1280\text{ cm}^{-1}$ , assigned to asymmetric vibration of T–O bond corresponding to external linkages between  $\text{TO}_4$  tetrahedra, is observed in all samples. However, peak near  $1590\text{ cm}^{-1}$ , corresponding to bending vibrations of adsorbed water molecules, is also present in all FTIR spectra of composites. The intensity of absorption peak, occurring at  $1109\text{ cm}^{-1}$ , is found to be decreasing with increase in

$\text{TiO}_2$  concentration and a broad absorption band at  $704\text{ cm}^{-1}$  disappears.

### 3.3 Ethanol sensing performance of the composite films

**3.3a Operating temperature and ethanol response:** Figure 4A and B shows the repeatability and reproducibility behaviour of metal oxide blended ZSM-5 composite sensors. Response to a fixed concentration of ethanol (100 p.p.m.) for ZnO/ZSM-5 films is depicted in figure 5a. Response to ethanol vapours by all composite film sensors shows a general trend, wherein the response to ethanol vapours goes on increasing with operating temperature and it reaches to a maximum value for a particular temperature. It decreases for further increase of operating temperature. It is also observed that the response decreases with the increase in subsequent trials, except for 50% ZnO concentration. These graphs indicate that the operating temperature for composite sensors, corresponding to maximum response, is a function of ZnO concentration. The ZnO/ZSM-5 composite film with 25% ZnO concentration is operated at comparatively lower operating temperature ( $90^\circ\text{C}$ ), as compared to sensors with 50 and 75% ZnO concentrations. It is further observed that for

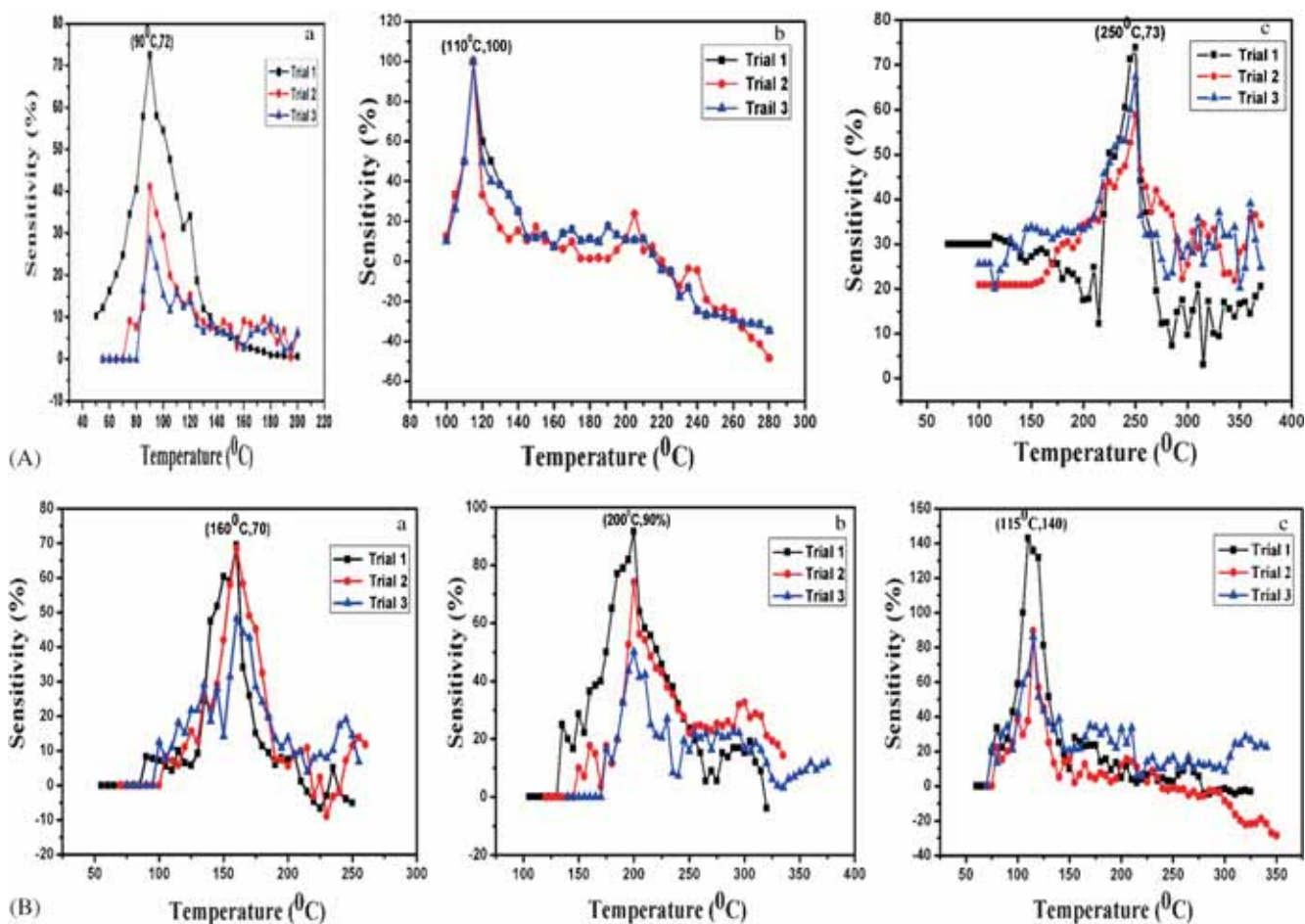


**Figure 4.** (A and B) Repeatability tests for ZnO/ZSM-5 and  $\text{TiO}_2/\text{ZSM-5}$  composite thick films showing the trend of change in sensitivity as a function of temperature: (a) 25% metal oxide, (b) 50% metal oxide and (c) 75% metal oxide.

higher ZnO concentration (75%), the operating temperature shifts to higher temperature (160°C).

Temperature dependence of the ethanol response of TiO<sub>2</sub>/ZSM-5 composite thick films is shown in figure 5b. The plots show similar kind of variation in ethanol response for all TiO<sub>2</sub> concentrations. The behaviour consists of increase in ethanol response with operating temperature, reaching to a maximum value followed by decrease in response with further increase in operating temperature. The operating temperature shows typical behaviour with respect to TiO<sub>2</sub> concentration. It changes from 160°C for 25% to 200°C for 50% and then suddenly shifts to 115°C for still

higher concentration of 75%. The study reveals that there is a strong influence of concentration of reinforcing material on operating temperature of blended ZSM-5 sensor matrix.

3.3b *Active region*: Figure 6a and b shows the change in ethanol response as a function of ethanol concentration for ZSM-5 and ZnO/ZSM-5 thick films held at their respective operating temperatures. The response increases rapidly in the lower concentration region of ethanol, while it increases gradually at higher concentrations of ethanol. It finally achieves a constant value for still higher ethanol concentration. The active region of the sensor is defined as

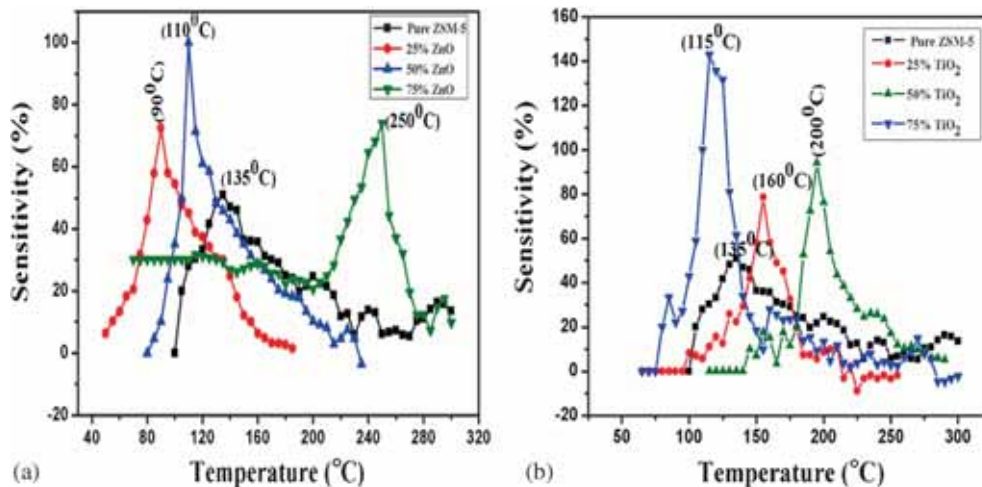


**Figure 5.** Comparative ethanol sensing behaviour of pure and metal oxide blended ZSM-5 composite thick film sensors showing the typical variation in operating temperature and sensitivity as a function of temperature: (a) ZnO/ZSM-5 and (b) TiO<sub>2</sub>/ZSM-5.

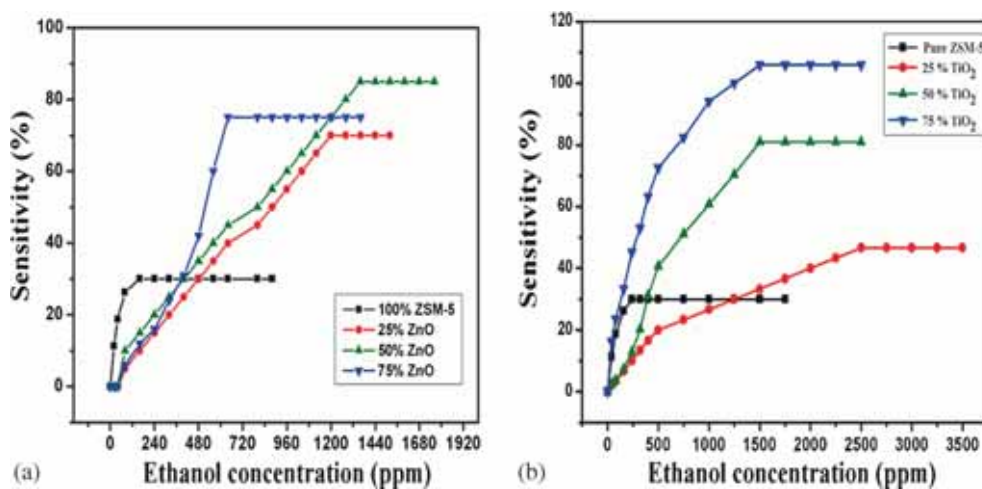


**Figure 6.** Comparative nature of ethanol uptake capacities of pure and metal oxide blended ZSM-5 composite thick film sensors as a function of ethanol vapour concentration. (a) ZnO/ZSM-5 at corresponding operating temperatures (90, 11 and 250°C) for 25, 50 and 75% of ZnO, respectively, and (b) TiO<sub>2</sub>/ZSM-5 at corresponding operating temperatures (160, 200 and 115°C) for 25, 50 and 75% of TiO<sub>2</sub>, respectively.

the range of ethanol concentration from particular minimum to maximum (p.p.m.) to which it can give response. Thus, the active regions for these composite sensors are found to be from 10 to 1200, 1360 and 640 p.p.m. at operating temperatures 90, 110 and 250°C for 25, 50 and 75% ZnO concentrations, respectively.

In the case of TiO<sub>2</sub>/ZSM-5 films, enhancement in ethanol sensing capability of sensor is observed and is depicted in figure 6b. However, the range of active region decreases with increase in TiO<sub>2</sub> concentration. The sensor with lowest TiO<sub>2</sub> concentration (25%) can sense the ethanol up to 2500 p.p.m. at an operating temperature 160°C. However, for higher concentrations (50 and 75% of TiO<sub>2</sub>), the ethanol uptake capacity for the sensor remains constant (1500 p.p.m.) at corresponding operating temperatures 200 and 115°C, respectively.

**3.3c Response/recovery behaviour:** Figure 7a presents the variation in response/recovery time for ZnO/ZSM-5

composite sensors as a function of ZnO concentration. It is clearly found that as the concentration of reinforcing ZnO increases, the corresponding composite film gives faster response upon exposure to ethanol and shows speedy recovery after exposing it to air.

The change in ethanol response as a function of time for TiO<sub>2</sub>/ZSM-5 sensors is shown in figure 7b. It is observed that all composite films give quick response to ethanol compared to that by pure ZSM-5 film sensor (150 s at 135°C). The composite film with 25% TiO<sub>2</sub> concentration results in quick response (10 s at 160°C), but takes longer time (200 s) to get recovered. The recovery time is found to be the lowest for 75 wt% TiO<sub>2</sub> (30 s at 115°C).

Figure 8A and B depicts the response/recovery transients for ZnO/ZSM-5 and TiO<sub>2</sub>/ZSM-5 composite sensors towards the ethanol vapours at respective working temperatures for variable concentration of ethanol. The ZnO/ZSM-5 composites with 25, 50 and 75% ZnO concentrations are operated

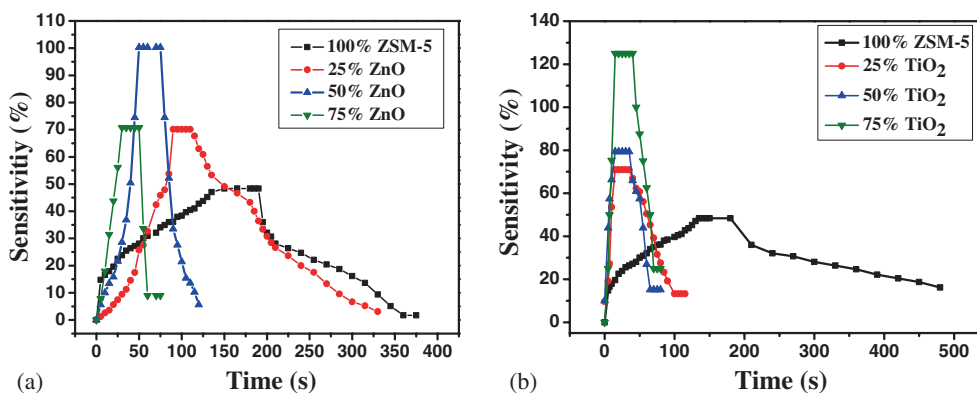


**Figure 7.** (a and b) Comparison of response and recovery behaviors of pure and metal oxide blended ZSM-5 composite thick film sensors as a function of time revealing the effect of metal oxide concentration. (a) ZnO/ZSM-5 at corresponding operating temperature (90, 110, 250°C) for 25, 50, 75% of ZnO, respectively, and (b) TiO<sub>2</sub>/ZSM-5 at corresponding operating temperature (160, 200, 115°C) for 25, 50, 75% of TiO<sub>2</sub>, respectively.

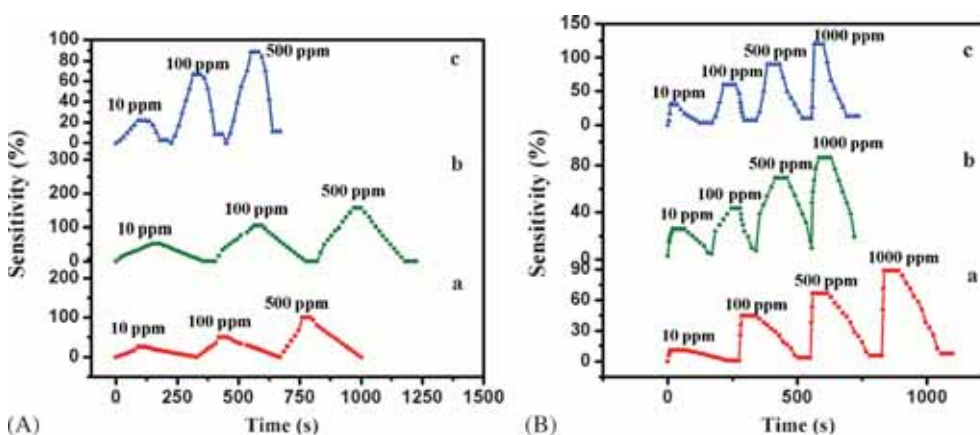


**Figure 8.** (A and B) Ethanol sensitivity of metal oxide blended ZSM-5 composite sensors upon exposure to ethanol at their respective operating temperatures demonstrating an increase in sensitivity with increase in ethanol concentration (A) ZnO/ZSM-5 at corresponding operating temperatures (90, 110, 250°C) for 25, 50, 75% of ZnO, respectively, and (B) TiO<sub>2</sub>/ZSM-5 at corresponding operating temperature (160, 200, 115°C) for 25, 50, 75% of TiO<sub>2</sub>, respectively.

**Table 1.** The ethanol sensing parameters of pure and ZSM-5 composite thick film sensors.

Materials	Pure ZSM-5	ZSM-5 + ZnO			ZSM-5 + TiO <sub>2</sub>		
		25% ZnO	50% ZnO	75% ZnO	25% TiO <sub>2</sub>	50% TiO <sub>2</sub>	75% TiO <sub>2</sub>
Operating temperature (°C)	135	90	110	250	160	200	115
Ethanol sensitivity (%)	50	72	100	75	70	97	140
Saturation (p.p.m.)	160	1200	1360	640	2500	1500	1500
Response time (s)	150	105	50	30	10	15	15
Recovery time (s)	180	185	60	30	200	80	30

at 90, 110 and 250°C, respectively. Likewise for 25, 50 and 75% TiO<sub>2</sub> concentrations, TiO<sub>2</sub>/ZSM-5 composites are operated at 160, 200 and 115°C, respectively. The typical ZnO/ZSM-5 sensor with 25% ZnO concentration (figure 8A(a)) shows response of the order of 25, 50 and 100 for 10, 100 and 500 p.p.m. concentrations of ethanol vapours, respectively. The ethanol response of TiO<sub>2</sub>/ZSM-5 sensor with the same concentration are found to be 11, 44, 66 and 88 for 10, 100, 500 and 1000 p.p.m., respectively. It can be concluded that the response goes on increasing with increase in ethanol vapour concentration for both types of blended films. The study reveals that all sensor films can sense ethanol vapours with a minimum concentration of 10 p.p.m. It is found that TiO<sub>2</sub>/ZSM-5 composite thick film sensor for 25% TiO<sub>2</sub> concentration can detect highly concentrated ethanol level of 2500 p.p.m. among all the composite sensors. The gas sensing parameters for these metal oxide blended zeolite composite sensors are summarized in table 1.

#### 4. Discussion

It is known that the ZSM-5 zeolite structure consists of two intersecting sets of tubular channels formed by a 10-membered ring of TO<sub>4</sub> tetrahedra [5]. Therefore, most probable sites offered by peculiar well-aligned ZSM-5 structure for guest molecules are straight channels, sinusoidal channels and a region of channel intersection (a nearly spherical cavity of 8.7 Å dia). Moreover, the internal microporosity of zeolites gives rise to high surface area, providing additional sites for adsorption of molecules to take place. In case of metal oxide blended ZSM-5 zeolites, metal oxides molecules, being nanoparticles, may occupy sites available inside the channels and also vacant sites available outside the channel, as shown in figure 9. As a result of incorporation of ZnO and TiO<sub>2</sub> nanoparticles in any of these sites, the surface area of the metal oxide blended ZSM-5 sensors increases [12]. Upon exposure of ethanol vapours, ethanol molecules can spread into the well-aligned structure very effectively resulting in larger interactions. Therefore, ZnO as well as TiO<sub>2</sub> blended ZSM-5 sensors show enhancement of ethanol sensitivity, which is shown in figure 9.

In pure ZSM-5, the conductivity is only due to mobile cations. Water molecules, present in the cages and channels,

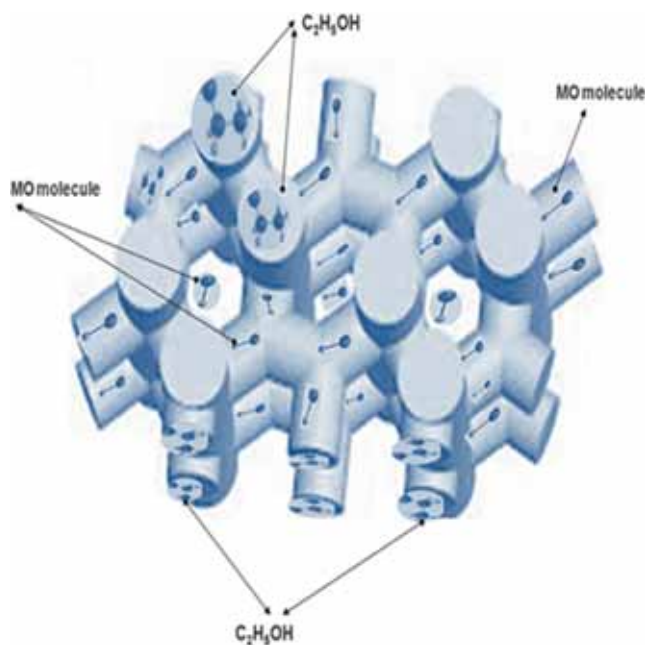
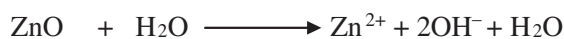


**Figure 9.** Schematic diagram of ZSM-5 zeolite channels with the incorporation of metal oxides (ZnO/TiO<sub>2</sub>) for ethanol sensing mechanism.

create hurdles for the motion of these cations. Therefore, conductivity is found to be low.

When ZnO or TiO<sub>2</sub> nanoparticles are encapsulated in ZSM-5, they may interact with the water molecules present in the void space of ZSM-5 zeolite and lead to protonation as follows [28–30]:



The interaction of water with ZnO surface results in partial dissociation of water molecule, resulting in H<sup>+</sup> and OH<sup>-</sup> species. The molecular adsorption of water on ZnO can be clearly identified by the presence of absorption band at 1590 and 3683 cm<sup>-1</sup> in FTIR spectra.

The formation of protons into the cages and channels of host ZSM-5 is equivalent to the H<sup>+</sup> form like zeolite structure. These protons may interact with the lone pair electron at

the hydroxyl group of the ethanol, leading to increase in conductivity. In other words, H<sup>+</sup> mobility or hopping of H<sup>+</sup> from one site to other may be responsible for enhanced conduction in case of composite sensor.

Furthermore, the ethanol vapours may possibly interact with lattice oxygen in metal oxide via the following reaction [31]:



Thus, in case of metal oxide blended ZSM-5 composites, not only cations and protons but also chemically adsorbed oxygen lattice sites, interact with ethanol vapour molecules. Therefore, the ethanol sensitivity is found to be higher than pure ZSM-5 zeolite for all composite sensors.

The dependence of sensitivities and operating temperature on the concentration of metal oxides may be due to the number of adsorption sites present for ethanol adsorption at that specific temperature for a particular concentration. In case of ZnO blended samples, maximum sensitivity is observed for 50% ZnO concentration. This may be due to the availability of sufficient ionic species of oxygen on the film surface along with protons which may interact most effectively with ethanol vapour molecules at that temperature. In case of TiO<sub>2</sub>, maximum sensitivity is observed for the highest TiO<sub>2</sub> concentration (75%). It may also be due to the availability of maximum adsorption sites at that concentration.

The gas upload capacity is determined by exposing the metal oxide blended sensor to variable concentrations of ethanol vapours. For a low ethanol concentration (10 p.p.m.), film surface area covered by the ethanol molecules is also small and hence the surface reactions between oxygen molecules, protons and ethanol molecules takes place slowly because of the availability of fewer number of ethanol molecules to react with and to get adsorbed. Increase in ethanol concentration results in increase in surface reaction due to larger surface coverage of ethanol molecules, which in turn leads to a rapid increase in ethanol response. On further increase in gas concentration, the surface coverage of ethanol molecules on the film begins to attain saturation. Hence, the response to ethanol saturates for higher ethanol concentrations.

Decrease in response time with increase in metal oxide concentration may also be related to availability of number of oxygen ion species to interact with ethanol molecules.

## 5. Conclusions

The introduction of ZnO and TiO<sub>2</sub> into ZSM-5, by physical dispersion method, does not alter the basic structure of ZSM-5 zeolite. Blending ZSM-5 zeolite with metal oxides enhances the sensor response to ethanol. Concentration of blended metal oxides has strong influence on ethanol sensing parameters like operating temperature, active region and response/recovery behaviour. Response decreases with increase in ZnO concentration, while it increases with

increase in TiO<sub>2</sub> concentration. These novel composite sensors can detect ethanol gas with a minimum concentration of 10 p.p.m. Higher ethanol uptake capability is observed for TiO<sub>2</sub> blended sensors than ZnO blended sensor. Introduction of metal oxides as reinforcing materials in ZSM-5 leads to fast response (to ethanol) and recovery. The study reveals that there is a strong influence of concentration of blended metal oxide materials on ethanol sensing behaviour of ZSM-5 zeolite.

## Acknowledgement

This work was carried out under the Major Research Project (F. No. SR/S2/CMP-49/2009) funded by the Department of Science and Technology (DST), New Delhi, India.

## References

- [1] Yang S, Lach-hab M, Vaisman I I, Blaisten-Barojas E, Li X and Karen V L 2010 *J. Phys. Chem. Ref. Data* **39** 033102
- [2] Xue Z, Ma J, Zheng J, Zhang T, Kang Y and Li R 2012 *Acta Mater.* **60** 5712
- [3] Sahner K, Hagen G, Schonauer D, Reis S and Moos R 2008 *Solid State Ionics* **179** 2416
- [4] Shirazi L, Jamshidi E and Ghasemi M R 2008 *Cryst. Res. Technol.* **43** 1300
- [5] Lu R, Tangbo H, Wang Q and Xiang S 2003 *J. Nat. Gas Chem.* **12** 56
- [6] Hagen G, Dubbe A, Rettig F, Jerger A, Birkhofer T, Müller R, Plog C and Moos R 2006 *Sensor Actuat. B Chem.* **119** 441
- [7] Dubbe A and Moos R 2008 *Sensor Actuat. B Chem.* **130** 546
- [8] Sazama P, Jirglová H and Dědeček J 2008 *Mater. Lett.* **62** 4239
- [9] Xu X, Wang J and Long Y 2006 *Sensors* **6** 1751
- [10] Zheng Y, Li X and Dutta P K 2012 *Sensors (Basel)* **12** 5170
- [11] Sun Y-F, Liu S-B, Meng F-L, Liu J-Y, Jin Z, Kong L-T and Liu J-H 2012 *Sensors (Basel)* **12** 2610
- [12] Zhang W, Bi F, Yu Y and He H 2013 *J. Mol. Catal. A Chem.* **372** 6
- [13] Dighavkar C 2013 *Arch. Appl. Sci. Res.* **5** 96
- [14] Patil D R, Patil L A and Amalnerkar D P 2008 *Bull. Mater. Sci.* **30** 553
- [15] Roy S, Saha H and Sarkar C K 2010 *Int. J. Smart Sens. Intell. Syst.* **3** 605
- [16] Mahabole M P, Lakhane M A, Choudhari A L and Khairnar R S 2012 *J. Porous Mater.* **20** 607
- [17] Cheng Y, Liao R H, Li J S, Sun X Y and Wang L J 2008 *J. Mater. Process. Technol.* **206** 445
- [18] Dayan N J, Sainkar S, Karekar R and Aiyer R 1998 *Thin Solid Films* **325** 254
- [19] Mene R U, Mahabole M P, Aiyer R C and Khairnar R S 2010 *Open Appl. Phys. J.* **3** 10
- [20] Khatamian M and Irani M 2009 *J. Iran Chem. Soc.* **6** 187
- [21] Ming C and Wu P 2005 *Chin. J. Geochem.* **24** 370
- [22] Karakassides M A 1997 *Clays Clay Miner.* **45** 649

- [23] Moreno-Piraján J C, Garcia-Cuello V S and Giraldo L 2010 *J. Thermodyn. Catal.* **1** 1
- [24] Nejati K, Rezvani Z and Pakizevand R 2011 *Int. Nano Lett.* **1** 75
- [25] Padilha R S, Ferrari-Lima A M, Seixas F L, Vagner R, Fávaro S L, Hioka N and Fernandes-Machado N R C 2013 *Chem. Engg. Trans.* **32** 823
- [26] Senthilkumar K, Paul P, Selvaraju C and Natarajan P 2010 *J. Phys. Chem. C* **114** 7085
- [27] Ba-Abbad M M, Kadhum A A H, Mohamad A B, Takriff M S and Sopian K 2012 *Int. J. Electrochem. Sci.* **7** 4871
- [28] Yimlamai I, Niamlang S, Chanthanont P, Kunanuraksapong R, Changkhamchom S and Sirivat A 2011 *Ionics (Kiel)* **17** 607
- [29] Zeng W, Liu T and Wang Z 2010 *Mater. Trans.* **51** 243
- [30] Baruah S, Pal S K and Dutta J 2012 *Nanosci. Technol.* **2** 90
- [31] Daryakenari A A, Vaezi M R, Ebadzadeh T and Daryakenari M A 2012 *Int. J. Phys. Sci.* **7** 2110